391

Impact of Leaf Area Index seasonality on the annual land surface evaporation in a global circulation model

Bart J.J.M. van den Hurk[1],
Pedro Viterbo and Sietse O. Los[2]

Research Department

November 2002

[1] Royal Netherlands Meteorological Institute, De Bilt, The Netherlands
[2] University of Wales, Swansea, UK

Submitted to J. Geophys. Res.

For additional copies please contact

The Library
ECMWF
Shinfield Park
Reading, Berks RG2 9AX

library@ecmwf.int

Series: ECMWF Technical Memoranda

A full list of ECMWF Publications can be found on our web site under:
http://www.ecmwf.int/publications.html

Abstract

Numerical experiments with the global model of the European Centre for Medium-Range Weather Forecasts (ECMWF) were devoted to the sensitivity of the modelled evaporation and precipitation to the vegetation Leaf Area Index (LAI). The temporally static LAI-distribution was replaced with a seasonally varying LAI, derived from Normalized Difference Vegetation Index (NDVI) archives. The seasonality of surface evaporation increased likewise, in combination with a response of increased precipitation seasonality over land.

In a second set of experiments, the LAI-estimates were perturbed by a noise term reflecting measurement accuracy and interannual variability. The resulting noise in evaporation and precipitation was compared to the noise intrinsically generated by the atmosphere. For periods and areas where evaporation forms a large term in the surface energy balance, the noise added to the LAI could be clearly discerned from the atmospheric noise, indicating that improved LAI-estimation techniques can have a detectable impact on the surface evaporation calculated in the ECMWF global model.

1 Introduction

The presence of vegetation has a significant effect on the regional and global hydrological cycle. Owing to its ability to extract water from deep soil reservoirs, it increases the hydrological 'memory' of the surface hydrological system. Furthermore, it intercepts a significant portion of precipitation, allowing for a rapid recycling of water by means of fast evaporation. Finally, vegetation is known to affect the surface albedo, thereby controlling the surface available energy. This important role of vegetation is acknowledged in most state-of-the art models used for Numerical Weather Prediction (NWP) and climate simulation (Dickinson *et al*, 1991; Garrat, 1993). In these models, vegetation is often characterized by the amount of (evaporating) leaf surface area per unit ground area, expressed as the Leaf Area Index (LAI). In most models the LAI is related to the efficiency of canopy evaporation by means of a so-called canopy conductance parameterization. High LAI values are correlated to high canopy conductance values, resulting in a relatively large portion of the available energy that is used for evapotranspiration (Brutsaert, 1982).

The LAI shows a clear spatial and temporal variation. Spatially it varies with the distribution of vegetation biomes across the globe, resulting in high values in tropical forest areas, moderate amounts for many agricultural and natural vegetation biomes at mid- to high latitudes, to low amounts in tundra and (semi-) desert areas. The most significant time scale is the seasonal variation of many vegetation biomes, which produce leaf tissue during periods when radiation and soil water allow biomass production (Wilson and Henderson-Sellers, 1985).

Since the late 1980s this spatial and temporal variability of LAI has been incorporated in NWP and climate models (e.g. Sellers *et al*, 1986; Koster and Suarez, 1992; Dickinson *et al*, 1993; Noilhan and Mahfouff, 1996). In these implementations, LAI values (either constant in time or with a seasonal variation) were assigned to broad vegetation classes by means of a look-up table, and spatial distributions of these vegetation types were specified from climatologies as from Wilson and Henderson-Sellers (1985) or Olson *et al* (1983). However, the interpretation of the vegetation types and associated parameter assignment may vary widely across modelling systems, and usually does not allow to incorporate inter-annual variability of vegetation intensity. As an alternative, Sellers *et al* (1996) and Los *et al* (2000) developed algorithms to retrieve necessary information on vegetation presence and phenology using operational satellite data, in particular using data from the Advanced Very High Resolution Radiometer (AVHRR) on board of the polar orbiting National Oceanic and Atmospheric Administration (NOAA) satellites. In spite of acknowledged difficulties in

the retrieval of accurate vegetation information from the relatively coarse resolution (1 × 1 km) AVHRR data (Leprieur *et al*, 1994), this approach accounts for interannual variability of vegetation and spatial patterns not captured in the fixed vegetation type climatologies (Buermann *et al*, 2001).

New satellite programs and increased understanding of the role of vegetation in the hydrological cycle enable the use of more realistic vegetation fields, such as LAI. An important issue is the assessment of the degree to which LAI measurements affects the hydrological cycle in a Atmospheric Global Circulation Model (AGCM). Fraedrich *et al* (2000) compared the hydrological cycle and atmospheric circulation patterns in the ECHAM4 climate model for a fully vegetated world (all land area fully covered with a dense vegetation pack) and for a desert world (no vegetation at all). In this comparison of extreme scenario's they found a significant intensification of the hydrological cycle and westerly flow patterns at the mid- and higher latitudes in the green-world simulations. Also less drastic sensitivity experiments with global circulation models illustrate the role of LAI in the partitioning of available energy over sensible and latent heat, the leaf interception and annual cycle of the soil water reservoir (Pielke *et al* 1997; Bounoua *et al*, 2000; Zeng and Neelin, 2000; Buermann *et al*, 2001). However, does the representation of a realistic seasonal cycle in LAI lead to significant changes in the hydrological cycle of an AGCM, compared to a LAI distribution remaining constant in time? And if so, are current accuracies of determining LAI from remote sensing observations adequate?

These questions are addressed in this study by a numerical simulation experiment using the AGCM of the European Centre for Medium-Range Weather Forecasts (ECMWF). The Land Surface Parameterization (LSP) of this AGCM makes use of a spatial LAI distribution fixed in time (Van den Hurk *et al*, 2000). Using the retrieval algorithm of Los *et al* (2000) a temporal evolution was incorporated in the LAI fields used in the ECMWF LSP. Simulations incorporating a full annual cycle were executed to determine the impact of this LAI seasonality on the land surface evaporation and global precipitation. In line with the methodology presented by Koster *et al* (2000), a small ensemble of simulations was executed to separate the signal from the noise in the results. In a second series of ensemble simulations, a noise term was added to the seasonal LAI values to mimic a (random) noise in the retrieval of LAI from remote sensing observations. The impact of this noise was compared to the variance generated by atmospheric noise to assess the degree to which the retrieval inaccuracy may be expected to affect the results of the AGCM. The study is limited to the direct hydrological effects of LAI, i.e. the control of the canopy transpiration and interception. Changes of surface albedo in response to LAI-changes may be significant, but were not considered here.

2 Methodology

2.1 Leaf Area Index in the ECMWF land surface scheme

The simulations in this study were carried out with an LSP scheme labelled TESSEL (Tiled ECMWF Surface Scheme for Exchange processes over Land), which is a component of the 1958-1998 ECMWF Reanalysis (ERA40). The scheme has been described and tested against results of a range of land surface measurement campaigns by Van den Hurk *et al* (2000), and is in operational use since June 2000. Common to many LSP's, TESSEL partitions available radiative energy over ground, sensible and latent heat flux by means of parameterizations of the exchange coefficients coupling the land surface to the deep soil and the atmosphere. In TESSEL, this surface energy balance is solved for up to 6 subgrid land-fractions: low and high vegetation, snow on low or under high vegetation, bare ground, and a vegetation interception reservoir. Vegetation types

are assigned to each grid box using the Global Land Cover Climatology (GLCC) from the US Department of Agriculture (USDA). This 1 × 1 *km* climatology is based on a combination of AVHRR data (April 1992 – March 1993), digital terrain models and supervised classification procedures (see http://edcdaac.usgs.gov/glcc/glcc.html. After a first classification into 94 biome types, grouping into a limited number of broad vegetation classes is applied. For the current study the first release (version 1.2) of GLCC has been used, with the vegetation type classification as defined for the Biosphere-Atmosphere Transfer Scheme (BATS) (Dickinson *et al*, 1993).

Each grid box of the model contains three specified fractions: a fraction C_H with a specified high vegetation type, a fraction C_L with a low vegetation type, and a fraction of bare ground. Both C_H and C_L are obtained as a combination of two factors: the grid box fraction of the specified vegetation type i, and a vegetation-type specific vegetation cover, $C_{veg}(i)$. Thus, grid boxes entirely occupied by vegetation type i are covered for a fraction $C_{veg}(i)$ with vegetation, the rest being bare ground. The snow and interception grid box fractions are dynamically calculated during the simulation. For each of the vegetation types a (fixed) LAI value is assigned from a look-up table. The total LAI of a grid box, LAI_T, is a linear combination of the LAI from the high and from the low vegetation type:

$$LAI_T = C_H LAI_H + C_L LAI_L \tag{1}$$

In TESSEL there is no distinction between total and green leaf matter: all leaf area in the model is assumed to be biologically active and contribute to the transpiration process.

2.2 2.2 Derivation of the seasonal Leaf Area Index fields

Los *et al* (2000) describe a procedure to calculate total LAI from Normalized Difference Vegetation Index (NDVI) data derived from AVHRR measurements. NDVI is considered to contain information on vegetation density by making use of the typical different reflectivity of visible and near-infrared radiation by canopy leaves. The procedure of Los *et al* (2000) includes corrections for sensor degradation, atmospheric aerosol and cloud effects, and solar zenith angle variations. A multiyear (1982-1990) dataset of biophysical quantities (including total LAI) is produced on a 1° × 1° grid on a monthly time scale. Input data consisted of the Global Area Coverage (GAC) 4 km resolution archive. Compared to other LAI datasets (for instance, Myneni *et al*, 1997) the current data set is based on a relatively long and continuous satellite data archive including corrections for a large number of processes known to affect the raw NDVI data. These multiyear total LAI estimates have been used to prescribe a seasonal cycle of the LAI-fields in the ECMWF global model as described below.

The use of global distributions of vegetation types in the ECMWF-model was kept intact. However, the (prescribed) constant LAI values were replaced by monthly varying values. These values were obtained by calibrating the monthly geographically distributed NDVI-based dataset (labelled LAI_N hereafter) on the vegetation types as used in the ECMWF global model. For each vegetation type, a selection of model gridboxes was made in which that vegetation type occupied more than 80% of the gridbox. A frequency distribution of the LAI_N-values in this selection of gridboxes was constructed, giving a range of possible LAI-values for each vegetation type. The values corresponding to the 80%-percentile of this frequency distribution appeared to generate a zonally averaged LAI-field that matched the zonal mean LAI_N-values very

well, and these values were assigned to the vegetation types. In this procedure, the calibration was applied separately to the northern and to the southern hemisphere, thus providing two LAI-values per vegetation type per month.

However, the LAI-values in the NDVI-database are assumed to represent the amount of leaf area per unit *total* ground area. In the ECMWF-model LAI-values are used to calculate the amount of leaf area per unit *vegetated* ground area, and are supposedly larger than the LAI_N-data. To remove this inconsistency, also the fraction of ground covered by vegetation for each vegetation type was obtained from the NDVI-data. In the approach of Los *et al* (2000) the vegetation cover is constant in time but a spatially varying parameter, related to the maximum NDVI-value in the season. A multi-linear regression was used to associate this spatially distributed vegetation cover with the ECMWF vegetation types. The use of a consistent combination of LAI and C_{veg} finally results in the amount of leaf area per unit grid box area given by

$$LAI_T = \sum_{i=low,high} C_i \, LAI_N / C_{veg}(i) \tag{2}$$

where the summation is over the low and high vegetation types, $C_{veg}(i)$ representing the recalibrated vegetation coverage, and with C_i the fraction of the grid box covered with vegetation type i (see Table 1). This procedure generates leaf area index distributions in the ECMWF model similar to the LAI_N-data by modifying both the *LAI* in the vegetated part of the ECMWF grid box and the fraction of grid box covered with vegetation. The change of the vegetation fraction may be associated with a change of the relative bare ground evaporation, in particular for grid boxes dominated by crops and short grass, where the modifications to C_{veg} where rather large.

Vegetation type	**C_{veg}**		**LAI**		
	Original	**New**	**Original**	**Min.**	**Max.**
Crops, Mixed Farming	0.9	0.179	3	0.69	3.36
Short Gras	0.85	0.356	2	0.41	1.78
Evergreen Needleleaf Trees	0.9	0.623	5	1.95	4.96
Deciduous Needleleaf Trees	0.9	0.609	5	0.08	5.54
Deciduous Broadleaf Trees	0.9	0.777	5	0.72	5.88
Evergreen Broadleaf Tree	0.99	0.889	6	4.89	5.14
Tall Grass	0.7	0.449	2	0.31	1.74
Desert	0.	0.	0.	0.	0.
Tundra	0.5	0.363	1	0.08	2.25
Irrigated Crops	0.9	0.569	3	0.64	1.79
Semidesert	0.1	0.203	0.5	0.4	0.87
Bogs and Marshes	0.6	0.365	4	0.88	4.50
Evergreen Shrubs	0.5	0.214	3	0.80	2.36
Deciduous Shrubs	0.5	0.595	1.5	0.43	1.35
Mixed Forest/woodland	0.9	0.827	5	1.02	6.68
Interrupted Forest	0.9	0.855	2.5	1.55	5.34

Table 1 Vegetation cover and LAI per vegetation type, in the original formulation of TESSEL (Van den Hurk et al, 2000), and recalibrated as to match the assumed cover in the NDVI-derived LAI-product. Only seasonal and combined northern & southern maximum and minimum LAI_N data are shown

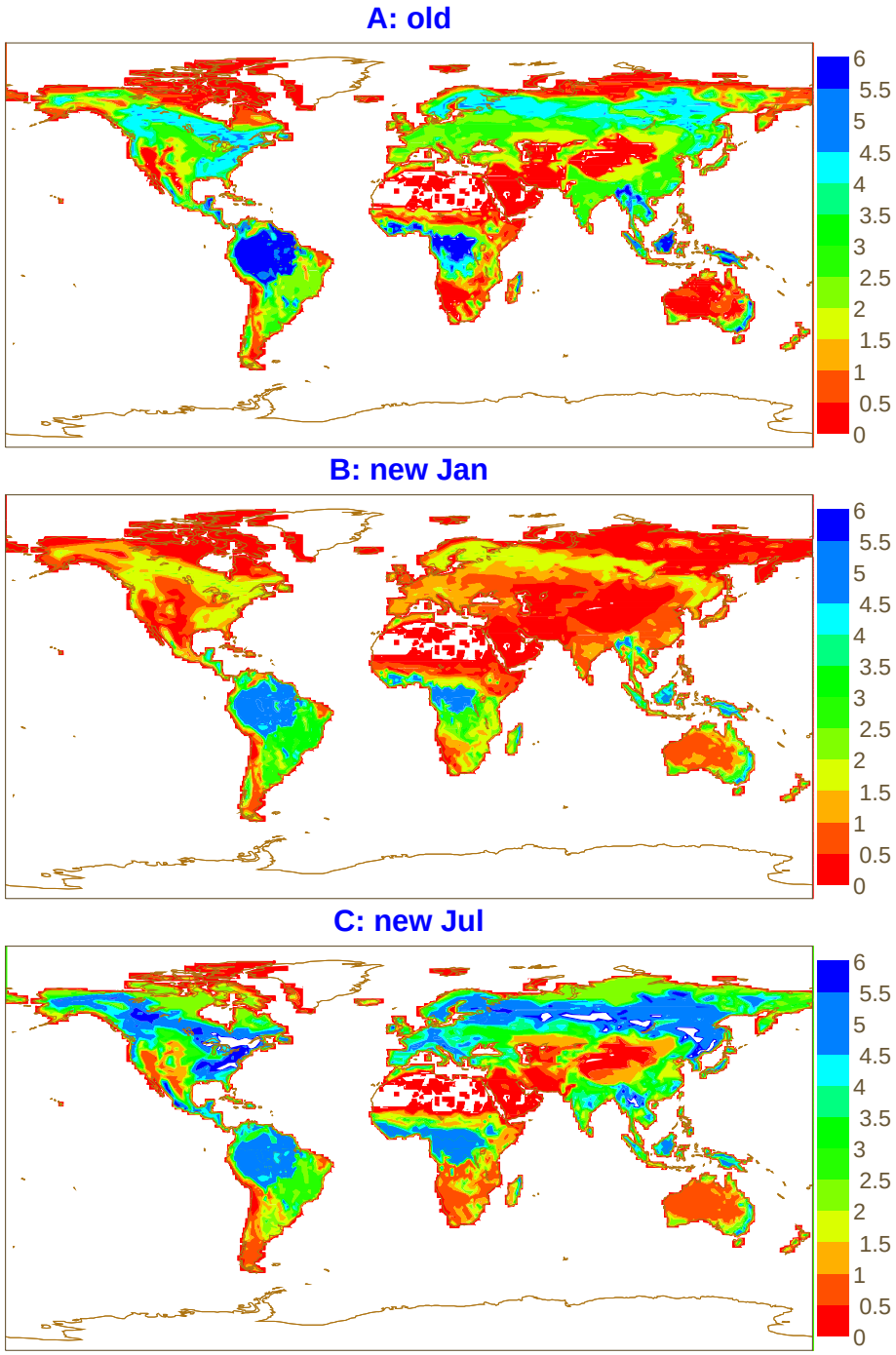

Figure 1 Global distribution of LAI (m2/m2) (Eq. 2) in the ECMWF-model, using a constant value throughout the year (A), and as obtained from the regression on LAIN estimates derived from NDVI data for January (B) and July (C).

This treatment of LAI does introduce a seasonal variation of the representation of vegetation in the TESSEL LSP, in common with many other surface schemes such as the Simple Biosphere Scheme (SIB; Sellers *et al*, 1996), BATS (Dickinson *et al,* 1993) and the Interaction Soil-Biosphere-Atmosphere (ISBA) scheme (Noilhan and Mahfouff, 1996). However, interannual vegetation variability (for instance induced by severe droughts

or large scale anthropogenic land use conversions) is not represented. This is why several LSP schemes under development use routine satellite data in combination with a dynamic vegetation development module to allow for frequent updates of the vegetation distributions.

To demonstrate the seasonality of the LAI thus obtained, Figure 1 shows the distribution of the LAI as defined by Equation 2 for the old situation without seasonality, and for the new distributions for January and July. Not only the areas dominated by crops or deciduous vegetation show a pronounced seasonality in the LAI, but also the areas dominated by "evergreen needleleaf trees" (for instance, large portions of the boreal forests) display significantly higher LAI values in summer than in winter. As may be expected, seasonality is limited in the tropical areas and the marginal vegetation areas in both the northern and southern hemispheres.

2.3 Model execution strategy

One may expect that this rather drastic change in the temporal evolution of LAI will be visible in the surface energy budget calculations (see below). However, of particular interest is the degree to which this seasonality results in a signal that can be distinguished from the noise that is inherently generated in an atmospheric circulation model. Therefore, simulations with the ECMWF model were executed by means of a small ensemble experiment.

The simulations were initiated between 1 and 5 January 1989, 12:00 UTC, and lasted approximately 13 months, until 1 February 1990. Results prior to 1 February 1989 (i.e. the first month) were discarded in the analyses in order to synchronize all ensemble members. A one year spin-up simulation was executed to generate the initial conditions of the soil moisture and temperature. Separate spin-up runs were executed for the control simulations (constant LAI) and the simulations using seasonally varying LAI (see below). The seasonal evolution of Sea Surface Temperature (SST) and sea ice cover were prescribed to the values used in the ECMWF 40-year reanalysis (ERA40). The atmospheric model was executed at a resolution of T159, whereas physical parameterization (including land surface processes) was operated at an approximately uniform gridpoint spacing of 112 km.

Three ensembles of five runs each were executed: a control ensemble using the original constant LAI values (labelled CLAI hereafter), an ensemble using the seasonal varying LAI-fields as described above (labelled SLAI), and an ensemble using the same seasonal LAI-fields modified by a noise term (labelled NLAI).

The generation of the "atmospheric noise"-ensemble in CLAI and SLAI was executed by initialising each run in these ensembles with a different atmospheric field, taken from atmospheric analyses of 1, 2, 3, 4 and 5 January 1989, 12:00 UTC. Monthly averages of each run were calculated from 1 February 1989 onwards.

A random noise term added to the LAI-fields in the NLAI ensemble was designed to represent both the accuracy of the retrieval of LAI from multi-annual NDVI-archives, and the lack of representation of interannual variability when using a fixed seasonal evolution of LAI. Inspection of interannual LAI-variability (Behrenfeld *et al*, 2001; Los *et al* 2001) in combination with detailed analysis of various errors in the retrieval procedures gives rise to suspect relatively larger errors for intermediate LAI-values during the transition between episodes with minimum and maximum leaf area. Estimation of the seasonal minimum and maximum is expected to be more accurate, owing to the limits in minimum and maximum possible plant biomass. In this experiment, the monthly LAI-values were modified by multiplying with a random number

taken from a Gaussian distribution with mean 1 and variance σ^2, ranging between σ^2_{min} = 10% and σ^2_{max} = 25% depending on the relative magnitude of the LAI in any given month *i*:

$$\sigma^2 = \sigma^2_{\min} + \frac{LAI_i - LAI_{\min}}{LAI_{med} - LAI_{\min}}\left(\sigma^2_{\max} - \sigma^2_{\min}\right) \qquad LAI_i < LAI_{med}$$

$$\sigma^2 = \sigma^2_{\max} + \frac{LAI_i - LAI_{med}}{LAI_{\max} - LAI_{med}}\left(\sigma^2_{\max} - \sigma^2_{\min}\right) \qquad LAI_i > LAI_{med} \tag{3}$$

with $LAI_{med} = 0.5(LAI_{\max} + LAI_{\min})$. No temporal or spatial consistency was retained in the random numbers generated: each vegetation type in each hemisphere was assigned a random multiplier for each month of the year. Modifications assigned to the dominant vegetation types provide a relatively strong contribution to the globally averaged LAI. Dominant vegetation types are the classes labelled "interrupted forest" (15% of vegetated land area in the ECMWF model), "short grass" (13%), "semi-desert" (11%), and "evergreen broadleef trees" (11%). This representation of noise in the LAI fields must be considered as a high estimate of the true accuracy of retrieval schemes such as the one presented by Los *et al* (2000). In these schemes temporal consistency and spatial organisation of vegetation types are inherent features that may affect the LAI-estimates in a systematic rather than in a random way.

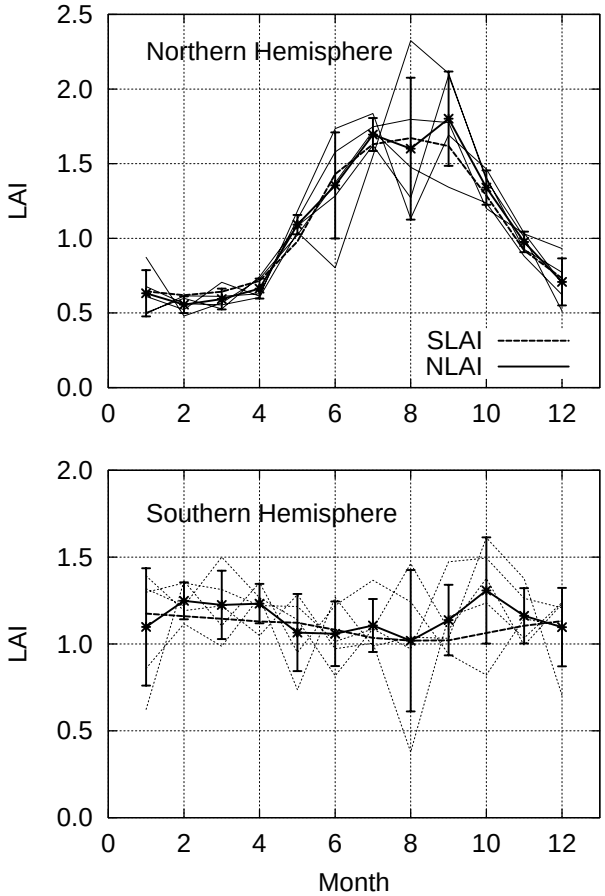

Figure 2 Monthly LAI averaged for the northern (top panel) and southern (bottom) hemispheres. Shown are the monthly mean values for all members of the NLAI ensemble (thin lines) and the averages for the SLAI and NLAI ensembles (thick lines). Vertical bars represent the standard deviation of the NLAI ensemble.

Each member of the NLAI-ensemble was initialized with the atmospheric analysis of 1 January 1989, but varied with respect to the monthly LAI-values assigned to each vegetation type. Figure 2 shows a time series of monthly averaged LAI for the SLAI and NLAI ensembles separately for the northern and southern hemispheres. In general the ensemble averages are within one standard deviation of the NLAI members, except for the northern hemisphere during winter, where the random noise assignment resulted in a slightly lower ensemble averaged leaf area index. The seasonality of LAI in the southern hemisphere is much less pronounced, as strong variation mainly occurs at land masses further away from the equator. However, the ensemble averaged LAI values remain within one standard deviation of the NLAI members.

3 Results

3.1 Seasonal versus constant LAI

As a baseline analysis, the seasonal cycle of evaporation over all land area in each of the southern and northern hemispheres is plotted for the CLAI and SLAI ensembles in Figure 3. Also shown in Figure 3 is the standard deviation of monthly evaporation calculated from the 5 members of each ensemble.

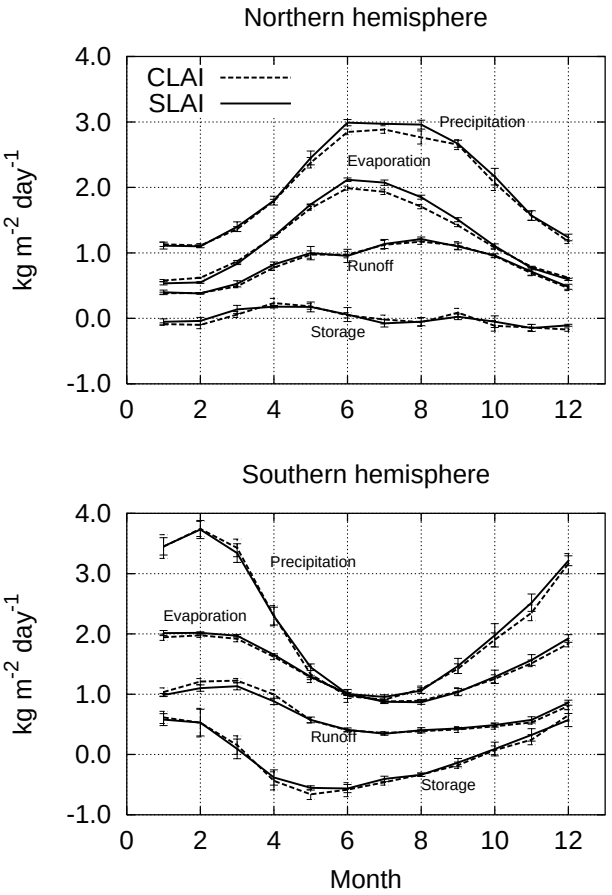

Figure 3 Time series of the monthly averaged components of the surface hydrological cycle averaged over land: precipitation, evaporation, runoff and soil moisture change (labelled storage). Results are shown separately for the northern (top) and southern (bottom) hemisphere, averaged for the fixed LAI (CLAI) and variable LAI (SLAI) ensembles. Also shown is the standard deviation of the values calculated for each of the ensembles.

The annual average evaporation over land is very similar for both ensembles: 1.28 $kg\ m^2\ day^{-1}$ for the CLAI experiment, 1.31 $kg\ m^{-2}\ day^{-1}$ for SLAI. However, the seasonality of the evaporation is modified, with lower evaporation rates in winter and higher in summer for the SLAI runs. In the months May to September the averaged land surface evaporation in the northern hemisphere are different by more than the ensemble standard deviations, pointing at a significant impact of the LAI seasonality on the land surface evaporation cycle in the ECMWF model. In the southern hemisphere the difference is less pronounced.

Land-averaged time series for the remaining surface water budget terms, i.e. precipitation, soil moisture change and runoff, are also shown in Figure 3. For clarity the snow budget has not been included in Figure 3, but the impact of the change in LAI on this term was fairly small. The increased land surface evaporation in the northern hemisphere in May – September results in a small increase in the total precipitation in this period, again differing by more than the ensemble standard deviations. Also in the southern hemisphere the change in land surface evaporation feeds back into a modified precipitation over land, rather than in a change in the other components of the surface hydrological budget.

A change in LAI affects the surface evaporation via two different processes: a change in the interception reservoir, and a modification of the canopy resistance regulating transpiration. Via the latter mechanism, an increased seasonal cycle of transpiration is linked to decreased soil moisture storage in the summer season. In the simulations shown here, this apparently is compensated by an increase in precipitation that enables the recharge of the soil reservoir on a time scale shorter than the seasonal cycle. A modification of the evaporation from intercepted precipitation does not affect the soil moisture content, and the response of evaporation to a change in LAI is therefore small.

Inspection of the spatial pattern in the change of the annual precipitation over land in response to a modification of the LAI fields reveals a strong spatial correlation with the distribution of vegetation types (which formed the entry to the spatial LAI-modification). Increased total annual precipitation occurred over areas covered with marginal vegetation types, mainly semi-desert, short grass, deciduous shrubland and tundra. Decreased annual precipitation was associated with areas dominated by agricultural crops and tropical forest.

3.2 Impact of uncertainty in LAI-retrieval

The analysis above has shown that land surface evaporation in the ECMWF model is clearly sensitive to the seasonal evolution of LAI. Global scale retrieval algorithms are able to estimate LAI values using satellite data with a limited accuracy.

It is relevant to establish whether noise on the LAI-estimates generates a detectable variance in the resulting evaporation fields. For that reason, a new simulation experiment was conducted, in which the noise generated by an inaccurate LAI-estimate is compared to the noise generated by using a range of separate initial atmospheric fields. The accuracy of the LAI-estimates is difficult to establish objectively, but here we applied a random noise to the LAI-fields from the SLAI ensemble resulting in an average variance between 10% and 25% (see Figure 2).

The quantity addressed is the ratio of the variance of evaporation over land induced by the variability in LAI, σ^2_{NLAI}, and the variance generated by the ensemble of initial atmospheric fields, σ^2_{SLAI}. Figure 4 shows a

Hovmöller diagram of the zonal means of $\sigma^2_{NLAI}/\sigma^2_{SLAI}$. Spatial patterns of the same quantity display a rather noisy longitudinal distribution but a clear north-south gradient. The zonal means are a logarithmic average of $\sigma^2_{NLAI}/\sigma^2_{SLAI}$ calculated for all gridboxes over land in 10° latitude bands. The logarithmic average is taken to avoid excessive contribution from gridboxes with extreme variance ratio values.

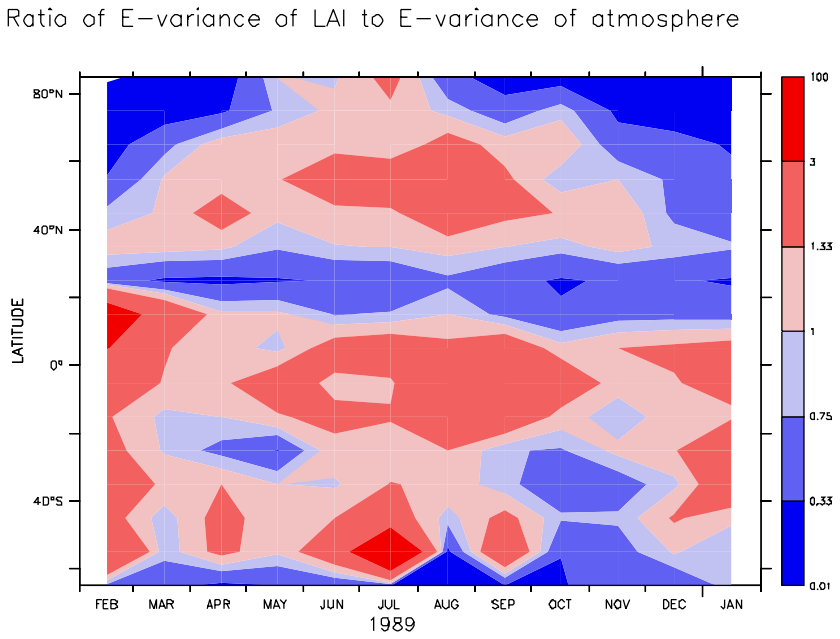

Figure 4 Hovmöller-diagram of zonal means of the ratio s $\sigma^2_{NLAI} / \sigma^2_{SLAI}$ as function of time in the year.

It is clearly seen that in the tropical zone around the equator a significant evaporation variance is generated by the LAI variability. Also during the NH growing season (May – August) a clear contribution of LAI variability is observed, but only outside the subtropics. Also in the southern hemisphere the variability is small in the subtropics. The pattern on the SH shows a less pronounced seasonal cycle, which is at least partially due to the relatively small amount of land grid points. This pattern suggests that the contribution of LAI variability is strongest in areas where evaporation uses a major fraction of the available energy: in the dry subtropical areas (in which LAI is generally also relatively low) relative changes of the low LAI values will not be able to induce large relative deviations of the evaporation, which is already constrained by a lack of available soil water.

At high latitudes and in winter at mid-latitudes LAI-variability does not give rise to strong changes of land surface evaporation. Here, limited radiative energy, snow processes and the influence of synoptic atmospheric activity rather than the amount of present leaf area dominate the evaporation process.

The strong correlation between changes in LAI and changes in local annual precipitation, as suggested in the previous section, is not evident from a Hovmöller diagram of the variance ratio of precipitation over land, shown in Figure 5. A spatially consistent pattern cannot easily be discerned, except a very small tendency of increased variance ratios with increasing distance from the equator.

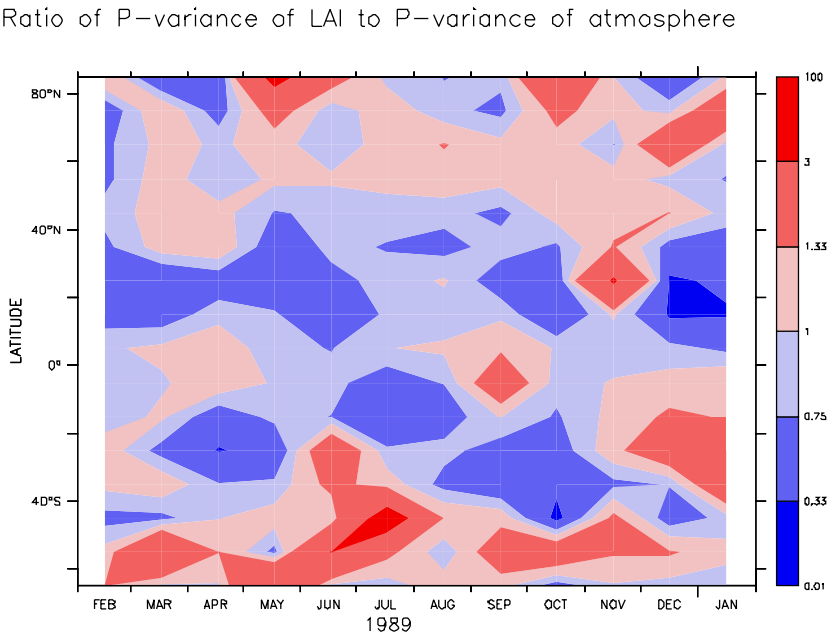

Figure 5 As figure 4, for the precipitation over land.

4 Discussion and conclusions

The work described in this paper explored the significance of imposing a seasonal cycle to the Leaf Area Index (LAI) in the land surface model of ECMWF. For a number of LAI-distributions, ensembles of five members each of one annual cycle were executed with the global model using analysed SST-fields and ice cover as forcing. The ensembles represented variability generated by both atmospheric noise and uncertainties in the LAI estimates.

The seasonal cycle of LAI, as derived from the estimates based on NDVI prepared by Los *et al* (2000), results in an increase of the range of the annual cycle of land surface evaporation: less evaporation in the winter season, and more in the summer. This is well understandable from the effect of the increased leaf area on partitioning of available energy over sensible and latent heat loss. For stressed evaporation conditions, an increase of LAI will favour the use of energy for evaporation. Also the enhanced recirculation of precipitation by evaporation of intercepted water is responsible for this positive correlation. The increase of evaporation can, on a climatological time scale, only be achieved when there is a compensating source of soil water, either by an increased precipitation or by a reduced loss of soil water by runoff and drainage. The results of the present study suggest that the main response is via the evaporation – precipitation feedback; no clear soil moisture spin-up effects were visible after the one year spin-up simulations. Annual cycles of soil moisture reservoir and runoff, averaged over the northern and southern hemispheres, were much less affected.

However, changes in the annual precipitation did not have the same sign everywhere. Precipitation increased over areas with marginal vegetation and decreased over cropland and tropical forest areas. Increased precipitation over semi-desert areas follows from an increase of both the average vegetation cover and the mean annual LAI (Table 1), but over short grass a decreased precipitation would have been expected given the strong *de*crease of both C_{veg} and LAI. However, this specific vegetation type is generally present in climate regions where precipitation is fairly evenly distributed over the year. This results in continuously

high soil water availability, enabling increased soil evaporation to compensate for reduced canopy transpiration. Decreased precipitation over areas dominated by crops and tropical forest may well be explained from reduced vegetation cover and mean annual LAI for these vegetation types.

Also the maximum depth of the annual cycle of soil moisture varied per region. In the operational application of the ECMWF model as a Numerical Weather Prediction system, soil moisture adjustments based on forecast errors of atmospheric humidity and temperature are applied routinely to correct for possible biases in evaporation, precipitation and runoff. The size of the average soil moisture correction may well be depending on the representation of the LAI, which is suggested by the presence of a clear annual cycle in these corrections (Douville *et al*, 2000).

Concerning the contribution of LAI-variability to variance of the surface evaporation, the results indicate that in areas and periods where land surface evaporation is significant, variability in the leaf area index can clearly be discerned from variability induced by atmospheric noise: around the equator in all seasons, and over mid latitudes in the northern hemisphere in the summer season. The conclusions are partially based on assumptions in the design of the experiment. For instance, the level of noise applied to the LAI-fields and the method of distributing this noise over time and space does not reflect the true accuracy with which LAI can eventually be estimated. Remote sensing algorithms generally have a temporal correlation in retrieval errors owing to the effect of assumptions in the algorithms that have a systematic impact on the estimates. This temporal consistency was not present in the current experiment. Also, the noise levels chosen are somewhat arbitrary, and could possible be justified better in the light of available remote sensing algorithms.

The results of this study may also be affected by potential biases in the satellite data. For instance, high latitude needle leaf forest vegetation may be impacted by low sun angles, mixture with deciduous trees, or snow in winter. This class is estimated by focusing on the NDVI value in October, where deciduous vegetation is dormant and snow cover is still relatively low. Similarly, biases may be introduced by assumptions needed to convert the satellite derived LAI data into parameters used in TESSEL. Consistent with TESSEL, we have used total LAI from the NDVI-based database assuming that all leaf area is biologically active. Admittedly, this assumption has a limited validity but uncertainties in the leaf area index are only partially responsible for the uncertainty in the estimate of canopy transpiration. In the land surface model explored here canopy transpiration is regulated by a canopy conductance, which depends on other factors such as sensitivity to light, soil water content, atmospheric humidity and a vegetation type specific maximum stomatal conductance. These variables were not changed in the simulations analysed here., For instance the choice of the value of the minimum stomatal conductance is also crucial, but difficult to determine. As demonstrated in this exercise, the uncertainty of LAI-estimates may contribute systematically to the variability of surface evaporation, but it only partially represents the total uncertainty of canopy parameters that regulate transpiration.

Also, the effects of LAI on the surface albedo were not included in this study: surface albedo varies seasonally over land, but in all simulations the same annual cycle of surface albedo was prescribed. A first order effect of LAI is to decrease the surface albedo with increasing leaf area. In general this decreased surface albedo may be expected to result in an increased evaporation rate, which implies an additional mechanism that increases evaporation with increasing LAI. The results found in this study would thus probably be enhanced if albedo changes had been allowed. Buermann *et al* (2001) concluded that this albedo

effect is smaller than the effect on the partitioning over sensible and latent heat in the NCAR Community Climate Model CCM3. Whether this is also the case for the ECMWF model used in the present study still needs to be confirmed.

The variation of LAI on the seasonal time scale affected the average seasonal cycle of precipitation over land, but noise applied to the LAI-estimate on a monthly basis was not clearly reflected in the precipitation variability on this time scale. This lack of response on the monthly time scale is strongly related to the spatial filtering of surface flux anomalies by the atmosphere. The noise added to the LAI-fields did retain the general seasonal cycle of the average LAI (see figure 2) by compensating LAI-increases in certain vegetation types at certain locations by decreases elsewhere.

The impact of variable LAI on precipitation variability can be considered as a superposition of the effect of two main mechanisms: a change of the (local) hydrological cycle, and a change of the atmospheric circulation patterns as a result of a modification of the spatial distribution of (latent) energy in the atmosphere. Each member of the experiment ensembles has a different atmospheric circulation pattern by design, but it has not been tested whether the leaf area index modification has a systematic effect on the circulation. It is difficult to draw firm conclusions on the relative role of these mechanisms because of the small ensemble size.

Koster *et al* (2000) analysed precipitation variability induced by variability in land surface fluxes using a similar procedure but mainly focussing at interannual variability. They found a strong local feedback between land surface processes and precipitation in the transition zones between subtropical and midlatitude areas, where the temporal precipitation distribution displays a strong seasonality. Repetitions of this analysis were carried out later with a suite of AGCM's, and the results of Koster *et al* (2000) appeared to be relatively strong compared to the other AGCM's involved in that later analysis (Koster *et al*, 2002). This implies that the nature of the land-atmosphere coupling in the regional and global hydrological cycle is still poorly understood. Future satellite missions devoted to land surface characteristics and lower atmosphere dynamics may prove helpful in increasing the understanding of this complex system.

5 Acknowledgements

This work has partially been sponsored by the European Space Agency under contract number 15164/01/NL/SF. Massimo Menenti provided valuable input to the work described. Three anonymous reviewers are acknowledged for their valuable comments on the manuscript.

6 References

Behrenfeld, M.J., J.T. Randerson, C.R. McClain, G.C. Feldman, S.O. Los, C.J. Tucker, P.G. Falkowski, C.B. Field, R. Frouin, W.E. Esaias, D.D. Kolber and N.H. Pollack (2001): Biospheric primary production during and ENSO transition; *Science* **291**, 2594-2597.

Bounoua, L. G.J. Collatz, S.O. Los, P.J. Sellers, D.A. Dazlich, C.J. Tucker and D.A. Randall (2000): Sensitivity of climate to changes in NDVI; *J. Climate* **13**, 2277-2292.

Brutsaert, W. (1982): *Evaporation into the atmosphere; theory, history and applications*; Reidel Publ.Comp., Dordrecht, The Netherlands; 299 pp.

Buermann, W., J. Dong, X. Zeng, R.B. Myneni and R.E. Dickinson (2001): Evaluation of the utility of satellite-based vegetation leaf area index data for climate simulations; *J. Climate* **14**, 3536-3551.

Dickinson, R.E., A. Henderson-Sellers, C. Rosenzweig and P.J. Sellers (1991): Evapotranspiration models with canopy resistance for use in climate models: a review; *Agr. For. Meteorol*. **54**, 373-388.

Dickinson, R.E., A. Henderson-Sellers and P.J. Kennedy (1993): Biosphere-Atmosphere Transfer Scheme (BATS) for the NCAR Community Climate model; *NCAR Technical Note* NCAR/TN-275+STR, 72 pp.

Douville, H., P. Viterbo, J.-F. Mahfouf and A.C.M. Beljaars (2000): Evaluation of the optimum interpolation and nudging techniques for soil moisture analysis using FIFE data; *Mon. Wea. Rev.,* **128**, 1733-1756.

Fraedrich, K., A. Kleidon and F. Lunkeit (1999): A green planet versus a desert world: estimating the effect of vegetation extremes on the atmosphere; *J.Climate* **12**, 3156-3163.

Garrat, J.R. (1993): Sensitivity of climate simulations to land-surface and atmospheric boundary-layer treatments - a review; *J. Climate,* **6**, 419-449.

Koster, R.D. and M.J. Suarez (1992): Modeling the land surface boundary in climate models as a composite of independent vegetation stands; *J.Geophys. Res*., **97**, 2697-2715.

Koster, R.D., M.J. Suarez and M. Heiser (2000): Variance and Predictability of Precipitation at Seasonal-to-Interannual Timescales; *J. Hydrometeorol*., **1**, 26-46.

Koster, R.D., P.A. Dirmeyer, A.N. Hahmann, R. IJpelaar, L. Tyahla, P. Cox and M.J. Suarez (2002): Comparing the degree of land-atmosphere interaction in four atmospheric general circulation models; *J. Hydrometeorol.,* **3**, 363-375.

Leprieur, C., M.M. Verstraete and B. Pinty (1994): Evaluation of the performance of various vegetation indices to retrieve vegetation cover from AVHRR data; *Remote Sensing Rev*., **10**, 265-284.

Los, S.O., G.J. Collatz, P.J. Sellers, C.M. Malmström, N.H. Pollack, R.S. DeFries, L. Bounoua, M.T. Parris, C.J. Tucker and D.A. Dazlich (2000): A global 9-year biophysical land-surface data set from NOAA AVHRR data. *Journal of Hydrometeorol*., **1**, 183-199.

Los, S.O., G.J. Collatz, L. Bounoua, P.J. Sellers and C.J. Tucker (2001): Global interannual variations in sea surface temperature and land surface vegetation, air temperature and precipitation; *J. Climate,* **14**, 1535-1549.

Myneni, R. B., R.Ramakrishna, R.Nemani and S. Running (1997): Estimation of global leaf area index and absorbed par using radiative transfer models. *IEEE Trans. Geosc. Rem. Sen*., **35**, 1380-1393.

Noilhan, J. and J.-F. Mahfouf (1996): The ISBA land surface parameterization scheme; *Global and Planetary Change,* **13**, 145-159.

Olson, J.S., J.A. Watts and L.J. Allison (1983): Carbon in life vegetation of major world ecosystems; ORNL-5862, Oak Ridge National Laboratory, Oak Ridge, USA.

Pielke, R.A., T.J. Lee, J.H. Copeland, J.L. Eastman, C.L. Ziegler and C.A. Finley (1997): Use of USGS-provided data to improve weather and climate simulations; *Ecol. Appl*., **7**, 3-21.

Sellers, P.J., Y. Mintz, Y.C.Sud, and A. Dalcher (1986): A simple biosphere model (SiB) for use within general circulation models; *J. Atmos. Sci*., **43**, 505-531

Sellers, P.J., S.O. Los, C.J. Tucker, C.O. Justice, D.A. Dazlich, G.J. Collatz and D.A. Randall (1996): A revised land surface parameterization (SiB2) for atmospheric GCM's. Part II: The generation of global fields of terrestrial biophysical parameters from satellite data; *J. Climate,* **9**, 706-737.

Van den Hurk, B.J.J.M., P. Viterbo, A.C.M. Beljaars and A.K. Betts (2000): Offline validation of the ERA40 surface scheme; *ECMWF TechMemo* No.295.

Wilson, M.F. and A. Henderson-Sellers (1985): A global archive of land cover and soils data for use in general circulation climate models; *J. Climatology,* **5**, 119-143.

Zeng, N. and J.D. Neelin (2000): The role of vegetation-climate interaction and interannual variability in shaping the African savanna; *J. Climate,* **13**, 2665-2670.